# Synthesis and Electronic Structure of Pentacyanoosmate(II) Complexes with N-Heterocyclic Ligands

**Leonardo D. Slep, Luis M. Baraldo, and José A. Olabe***

Departamento de Química Inorgánica, Analítica y Química Física (Inquimae), Facultad de Ciencias Exactas y Naturales, Universidad de Buenos Aires, Pabellón 2, Ciudad Universitaria, Capital Federal 1428, República Argentina

*Received April 4, 1996*[⊗]

The series of complexes $[Os^{II}(CN)_5L]^{n-}$, with L = pyridine or pyrazine derivatives, were prepared in aqueous solution and, in some cases, as sodium or potassium salts. The main feature in the UV−visible spectra is the appearance of an intense, asymmetric MLCT band, split under spin−orbit coupling. The energies and intensities of the MLCT bands decrease and increase, respectively, with the electron-acceptor ability of L, and strong solvatochromic energy shifts are observed in different organic media. The Os(II) complexes can be oxidized chemically or electrochemically to the Os(III) species; the latter show typical LMCT bands in the visible region, independent of L. The redox potentials for the $Os^{III,II}$ couples (range 0.6−1.0 V (NHE)), shift positively when L becomes more electron-withdrawing or less basic. Reduction potentials for the bound and free $Mepz^+$ ligand showed similar values, ca. −0.53 V (NHE), for the three $[M(CN)_5L]^{n-}$ complexes, suggesting similar back-bonding abilities of Fe, Ru, and Os toward a given L ligand; this is confirmed by the linear plots with unit slope obtained for the energy of the MLCT bands of the $[M(CN)_5L]^{n-}$ complexes (M = Fe, Ru) against the values for the $[Os(CN)_5L]^{n-}$ complexes. The IR spectra show intense and weak bands at ca. 2050 and 2100 $cm^{-1}$, associated with equatorial and axial cyanide stretchings, respectively. The dissociation rate constant for pyrazine release from the $[Os(CN)_5pz]^{3-}$ ion shows a saturation kinetic behavior, typical of dissociative mechanisms found for the iron and ruthenium analog complexes; the specific dissociation rate constant, $k_{-pz} = 2.0 \times 10^{-8}$ $s^{-1}$ (25 °C, $I$ = 0.5 M), is about 3 and 4 orders of magnitude slower than the values found for $[Ru(CN)_5pz]^{3-}$ and $[Fe(CN)_5pz]^{3-}$, respectively; this is ascribed mainly to the strong $\sigma$ interaction in the Os−L bond.

## Introduction

The chemistry of pentacyano(L)ferrate(II) complexes has received considerable attention because of the variety of L ligands able to bind to the $Fe(CN)_5^{3-}$ moiety ($H_2O$, $NH_3$, amines, phosphines, sulfite, nitrite, NO, CO, N-heterocyclic molecules, etc.).[1,2] Mechanistic studies on the ligand-interchange reactions have been carried out,[3−7] as well as on electron transfer reactions with the $[Fe^{II}(CN)_5L]^{n-}$ ions. The chemistry of mixed-valence binuclear complexes containing $Fe^{II,III}(CN)_5$ as one of the fragments has also been explored.[8] The most relevant aspects of this interesting chemistry have been reviewed.[2]

Studies on the related pentacyano(L)ruthenate complexes were developed more recently.[9−12] Only a few reports on the pentacyano(L)osmate ions exist in the literature,[1] including the studies on the hexacyanoosmate species[13] and the recently reported nitrosyl derivative $Na_2[Os(CN)_5NO]\cdot 2H_2O$.[14]

The need for synthesizing other members of the $[Os(CN)_5L]^{n-}$ series stems from the importance of performing systematic studies on the electronic structure and reactivity for analogous species with metal centers pertaining to the three transition series. The subject of the $\sigma-\pi$ interactions of the L ligands with different metal centers and the role of the coligands in controlling the electronic structure and reactivity of the M−L bonds has been considered in the available studies with the pentaammine[15] and pentacyano complexes.[2,9]

* Corresponding author. Telefax: 54-1-7820441. e-mail: olabe@ayelen.q3.fcen.uba.ar.

[⊗] Abstract published in *Advance ACS Abstracts,* September 1, 1996.

(1) Sharpe, A. G. *The Chemistry of Cyano Complexes of the Transition Metals*; Academic Press: New York, 1976; Chapter VII.
(2) Macartney, D. H, *Rev. Inorg. Chem.* **1988**, *9*, 101.
(3) Toma, H. E.; Malin, J. M. *Inorg. Chem.* **1973**, *12*, 1039.
(4) Toma, H. E.; Malin, J. M. *Inorg. Chem.* **1973**, *12*, 2080.
(5) Stochel, G.; Chatlas, J.; Martínez, P.; van Eldik, R. *Inorg. Chem.* **1992**, *31*, 5480.
(6) Haim, A. *Comments Inorg. Chem.* **1985**, *4*, 113 and references therein.
(7) (a) Haim, A. *Prog. Inorg. Chem.* **1983**, *30*, 273 and references therein. (b) Burewicz, A.; Haim, A. *Inorg. Chem.* **1988**, *27*, 1611. (c) Yeh, A.; Haim, A. *J. Am. Chem. Soc.* **1985**, *107*, 369. (d) Olabe, J. A.; Haim, A. *Inorg. Chem.* **1989**, *28*, 3278. (e) Huang, H. Y.; Chen, W. J.; Yang, C. C.; Yeh, A. *Inorg. Chem.* **1991**, *30*, 1862. (f) Sasaki, Y.; Ninomiya, T.; Nagasawa, A.; Endo, K.; Saito, K. *Inorg. Chem.* **1987**, *26*, 2164.
(8) Creutz, C. *Prog. Inorg. Chem.* **1983**, *30*, 1.
(9) (a) Johnson, C. R.; Shepherd, R. E. *Inorg. Chem.* **1983**, *22*, 1117. (b) Johnson, C. R.; Shepherd, R. E. *Inorg. Chem.* **1983**, *22*, 2439. (c) Olabe, J. A.; Gentil, L. A.; Rigotti, G. E.; Navaza, A. *Inorg. Chem.* **1984**, *23*, 4297.
(10) (a) Siddiqui, S.; Henderson, W. W.; Shepherd, R. E. *Inorg. Chem.* **1987**, *26*, 3101. (b) Henderson, W. W.; Shepherd, R. E. *Inorg. Chem.* **1985**, *24*, 2398.
(11) (a) Hoddenbagh, J. M. A.; Macartney, D. H. *Inorg. Chem.* **1986**, *25*, 380. (b) Hoddenbagh, J. M. A.; Macartney, D. H. *Inorg. Chem.* **1986**, *25*, 2099. (c) Hoddenbagh. J. M. A.; Macartney, D. H. *Inorg. Chem.* **1990**, *29*, 245.
(12) (a) Gentil, L. A.; Zerga, H. O.; Olabe, J. A. *J. Chem. Soc., Dalton Trans.* **1986**, 2731. (b) Olabe, J. A.; Zerga, H. O.; Gentil, L. A. *J. Chem. Soc., Dalton Trans*. **1987**, 1267. (c) Almaraz, A. E.; Gentil, L. A.; Olabe, J. A. *J. Chem Soc., Dalton Trans.* **1989**, 1973. (d) Chevalier, A. E.; Gentil, L. A.; Olabe, J. A. *J. Chem. Soc., Dalton Trans.* **1991**, 1959.
(13) (a) Gentil, L. A.; Navaza, A.; Olabe, J. A.; Rigotti, G. E. *Inorg. Chim. Acta* **1991**, *179*, 89. (b) Forlano, P.; Baraldo, L. M.; Olabe, J. A.; Della Vedova. C. O. *Inorg. Chim. Acta* **1994**, *223*, 37. (c) Macartney, D. H. *Inorg. Chem.* **1991**, *30*, 3337.
(14) Baraldo, L. M.; Bessega, M. S.; Rigotti, G. E.; Olabe, J. A. *Inorg. Chem.* **1994**, *33*, 5890.

S0020-1669(96)00377-1 CCC: $12.00 

## Experimental Section

**Materials.** $Na_2[Os(CN)_5NO]\cdot 2H_2O$ was prepared as described previously.[14] The potassium salt was obtained through cation interchange by an intermediate precipitation of the silver salt, as described elsewhere.[16] Anal. Calcd for $K_2[Os(CN)_5NO]\cdot H_2O$: C, 13.45; H, 0.45; N, 18.83. Found: C, 13.76; H, 0.24; N, 18.49. Potassium hexacyanoosmate(II) was prepared similarly to potassium hexacyanoruthenate.[17] Potassium pentacyano(*N*-methylpyrazinium)ruthenate was obtained through an adaptation of published procedures,[12] starting from the nitrosyl derivative.[18] Sodium pentacyano(*N*-methylpyrazinium)-ferrate, *N*-methylpyrazinium ($Mepz^+$) iodide, 1-methyl-4,4′-bipyridinium ($Mebpy^+$) iodide, and pyrazine *N*-oxide (pzO) were prepared by literature methods.[3,19−21] Anal. Calcd for MepzI: C, 27.05; H, 3.18; N, 12.62. Found: C, 27.14; H, 3.18; N, 12.51. Calcd for MebpyI: C, 44.32; H, 3.72; N, 9.40. Found: C, 44.29; H, 3.77; N, 9.40. Hydrazine hydrate (99%, Roth) was used as supplied. Other ligands used for coordination to $[Os(CN)_5]^{3-}$ were purchased from Aldrich and were used as supplied. Other chemicals were of analytical grade. In all the aqueous solution experiments, distilled water was deionized with Milli-Q equipment. The solvents (methanol, ethanol, acetonitrile, dimethylformamide) were of anhydrous, spectroscopic grade and were used without further purification.

**Preparation of the Solid Pentacyano(L)osmate(II) Complexes, L = pz, dmpz, $Mepz^+$, 4-CNpy, bpy, $Mebpy^+$. Method 1.** $Na_2[Os(CN)_5NO]\cdot 2H_2O$ (200 mg, 0.5 mmol)[14] was dissolved in 40 mL of water, in a stoppered plastic flask; 10 mL of 3 M NaOH and 400 mg (5 mmol) of pyrazine were added, and the mixture was held at 65 °C. As $[Os(CN)_5pz]^{3-}$ was produced, the solution turned from pale yellow to intense orange; the progress of the reaction was monitored spectrophotometrically at 386 nm. Upon completion (72 h), the mixture was cooled and slowly neutralized with a solution of 1 M HCl. The volume was reduced to 5 mL (rotavap, 25 °C), and the residue was poured onto a Sephadex G-25 column (length 1.5 m; width 2.5 cm), eluting with water. The fractions containing the desired product were concentrated, and the separation was repeated. The volume of the eluate was reduced to 2 mL, and the product was precipitated by adding 20 mL of cold acetone. The collected solid (glass frit No. 4) was washed with acetone and diethyl ether and dried over silica gel. Weight obtained: 132 mg. Anal. Calcd for $Na_3[Os(CN)_5pz]\cdot 3H_2O$: C, 20.65; H, 1.93; N, 18.74; Na, 13.18. Found: C, 20.67; H, 2.24; N, 18.69; Na, 13.3. The solids with L = dmpz and bpy were prepared by the same technique; in the latter case, the potassium salt was obtained by using $K_2[Os(CN)_5NO]\cdot H_2O$ and KOH. Anal. Calcd for $Na_3[Os(CN)_5$-dmpz$]\cdot 3H_2O$: C, 23.96; H, 2.40; N, 17.78. Found: C, 24.14; H, 2.40; N, 17.32. Calcd for $K_3[Os(CN)_5bpy]\cdot 2H_2O$: C, 28.61; H, 1.92; N, 15.57. Found: C, 29.39; H, 2.11; N, 15.12.

**Method 2.** $K_4[Os(CN)_6]$ (282 mg, 0.56 mmol) was dissolved in water (50 mL), and the solution was photolyzed under constant stirring during 26 h ($\lambda$ = 254 nm, pH 4, same experimental arrangement as described in ref 14, but without addition of nitrite); *N*-methylpyrazinium iodide (600 mg, 2.7 mmol) and ascorbic acid (500 mg) were added to the resulting green solution; after 24 h, the volume was reduced to 5 mL (rotavap, 25 °C) and the excess potassium hexacyanoosmate was precipitated with cold acetone. As the colored solid contained some of the desired $Mepz^+$ complex, it was washed successively with methanol. The collected fractions were mixed and evaporated to dryness, and the residue was dissolved in water (25 mL). $AgNO_3$ was added to precipitate the silver salt of the complex. The solid was filtered off (glass frit No. 4) and redissolved in a solution containing a slight defect of NaI. AgI was removed by filtering through a cellulose membrane (pore 0.02 $\mu$m). The filtrate was evaporated to dryness, and the solid so obtained was stored over silica gel. Weight: 87 mg. Anal. Calcd for $Na_2[Os(CN)_5Mepz]\cdot 4H_2O$: C, 22.51; H, 2.83; N, 18.38. Found: C, 22.75; H, 2.68; N, 17.86. The solids containing $Mebpy^+$ and 4-CNpy were also obtained through the latter technique, with a slight modification: after elimination of the excess hexacyanoosmate reactant, the potassium salts were precipitated by the addition of ethanol (for $Mebpy^+$) and acetone (for 4-CNpy). Anal. Calcd for $K_2[Os(CN)_5Mebpy]\cdot 4H_2O$: C, 29.94; H, 2.98; N, 15.28. Found: C, 29.39; H, 3.12; N, 15.57. Anal. Calcd for $K_3[Os(CN)_5$4CNpy$]\cdot H_2O$: C, 23.60; H, 1.08; N, 17.52. Found: C, 24.11; H, 0.93; N, 16.85. Elemental analyses (C, H, N) were performed with a Carlo Erba EA 1108 analyzer; sodium and potassium determinations were performed by atomic emission with a Varian 70 spectrometer.

**Preparation of the Complexes in Aqueous Solutions.** Three independent procedures were employed for the preparation of solutions (ca. $10^{-3}$ M) of the different complexes.

(a) A solution of pentacyanonitrosylosmate(II) was allowed to react with hydroxide, in the presence of the entering L ligand. This was performed by using the relative concentrations described in method 1; the procedure was successful with L = pz, 2-Mepz, dmpz, pdz, py, 3-Mepy, and 4-Mepy, but it could not be employed with L = $Mepz^+$, $Mebpy^+$, and isn, which were unstable in alkaline media.

(b) A mixture of pentacyanonitrosylosmate(II) and hydrazine hydrate (1:100) was left for reaction up to 24 h; after addition of glacial acetic acid (pH 6), an excess of the L ligand (10:1 with respect to osmium) was added and the mixture was held at 65 °C for 72 h. This procedure was useful for the complexes with unstable L ligands.

(c) Solutions of $K_2[Os(CN)_5N_2H_5]\cdot 2H_2O$ and L (10-fold excess) were mixed. The solid reactant was prepared as follows: To a solution of $K_2[Os(CN)_5NO]\cdot H_2O$ (50 mg) in methanol (25 mL), previously deaerated with argon, were added hydrazine hydrate (2 mL) and KI (25 mg); the initial yellow solution became colorless, and a white precipitate appeared; the solid was filtered off (glass frit No. 4) under argon and dried over silica gel. Anal. Calcd for $K_2[Os(CN)_5N_2H_5]\cdot 2H_2O$: C, 12.84; H, 1.94; N, 20.97; K, 16.72. Found: C, 12.92; H, 2.03; N, 21.23; K, 16.9. The solid was unstable, showing signs of decomposition within a few days, even when stored under vacuum.

The consistency of procedures a−c was checked by measuring the molar absorbance values for the pyrazine complex. For the three cases, the values were in agreement (within 3−5% error) with the one obtained through dissolution of the pure solid.

Solutions of the pyrazine complex in some organic solvents (methanol, ethanol, acetonitrile, dimethylformamide) were prepared by dissolving the sodium compound with the aid of complexing reagents (18-crown-6; Kriptofix 222). All the solutions were handled under argon to avoid the presence of water.

**General Procedures.** Ultraviolet and visible spectra were recorded with a Hewlett-Packard 8452A diode-array spectrophotometer. Molar absorbances were obtained either by dissolution of the solids or by preparing solutions of known concentration as described before. If the overlap with the spectrum of the free ligand was important, the complexes were purified by means of a Sephadex G 10 column ($l$ = 25 cm, $d$ = 2.5 cm). The entire spectrum obtained after the purification step, together with the one at quantitative concentration obtained in the presence of the free ligand, allowed for the calculation of the molar absorbance at any wavelength. IR spectra were taken in KBr pellets on a Nicolet 510P FTIR instrument. Cyclic voltammetry measurements were performed with a Princeton Applied Research 273A instrument, by using a cell with a three-electrode arrangement at sweep rates varying from 50 to 200 mV/s; a platinum disk was used as the working electrode and a platinum net as the counter electrode, with a standard Ag/AgCl electrode as reference. A glassy carbon working electrode was used for the oxidation processes around 1.0 V. A hanging drop Hg electrode (EG&G PARC Model 303A SMDE) was used for the reduction of bound $Mepz^+$ in the $[M(CN)_5Mepz]^{2-}$ complexes (M = Fe, Ru, Os) as well as for reduction of free $Mepz^+$ iodide. In all cases, the measurements were carried out under argon, with millimolar aqueous solutions of the complexes, at 25 °C, $I$ = 0.1 M ($NaNO_3$), unbuffered medium. Spectroelectrochemical measurements for the oxidation of Os(II) to Os(III) were carried out with a specially designed cell,

(15) (a) Ford, P. C. *Coord. Chem. Rev.* **1970**, *5*, 75. (b) Taube, H. *Surv. Prog. Chem.* **1973**, *6*, 1. (c) Taube, H. *Pure Appl. Chem.* **1979**, *51*, 901. (d) Taube, H. *Comments Inorg. Chem.* **1981**, *1*, 17. (e) Lay, P. A.; Harman, W. D. *Adv. Inorg. Chem.* **1991**, *37*, 219.
(16) Amalvy, J. I.; Varetti, E. L.; Aymonino, P. J.; Castellano, E. E.; Piro, O. E.; Punte, G. *J. Crystallogr. Spectrosc. Res.* **1986**, *16*, 537.
(17) Krause, R. A.; Violette, C. *Inorg. Chim. Acta* **1986**, *113*, 161.
(18) Waldhoer, E.; Slep, L. D.; Olabe, J. A.; Kaim, W.; Fiedler, J. To be submitted.
(19) Bahner, C. T.; Norton, L. L. *J. Am. Chem. Soc.* **1950**, *72*, 2881.
(20) Figard, J. E.; Paukstelis, J. V.; Petersen, J. D. *J. Am. Chem. Soc.* **1977**, *99*, 8417.
(21) Koelsch, C. P.; Gumprecht, H. *J. Org. Chem.* **1958**, *23*, 1603.

**Table 1.** MLCT Absorption Data for $[M^{II}(CN)_5L]^{n-}$ Complexes (M = Fe, Ru, Os) with L = Substituted Pyridine and Pyrazine Ligands[a]

| | | Fe | | Ru | | Os | | | | |
|---|---|---|---|---|---|---|---|---|---|---|
| no. | ligand | $\lambda$ (nm) | $\nu$ ($10^3$ $cm^{-1}$) | $\lambda$ (nm) | $\nu$ ($10^3$ $cm^{-1}$) | $\lambda_{max}$ (nm) | $\epsilon_{max}$ ($M^{-1}$ $cm^{-1}$) | $\nu_{max}$[b] ($10^3$ $cm^{-1}$) | $\nu_1$[c] ($10^3$ $cm^{-1}$) | $\nu_2$[c] ($10^3$ $cm^{-1}$) |
| **1** | 4-Mepy | 356 | 28.1[d] | 310 | 32.3[e] | 308 | 6090 | 32.5 | 32.7 | 28.4 |
| **2** | 3-Mepy | 362 | 27.6 | 308 | 32.5[f] | 316 | 5150 | 31.6 | 31.8 | 27.5 |
| **3** | py | 362 | 27.6[d] | 316 | 31.6[e] | 318 | 5460 | 31.4 | 31.5 | 27.1 |
| **4** | 3-CNpy | 414 | 24.2[g] | 340 | 29.4[h] | 354 | 5560 | 28.2 | 28.4 | 23.4 |
| **5** | bpy | 432 | 23.2[d] | 365 | 27.4[e] | 374 | 7770 | 26.7 | 27.0 | 22.9 |
| **6** | isn | 435 | 23.0[d] | 364 | 27.5[e] | 378 | 6220 | 26.5 | 26.8 | 22.5 |
| **7** | 4-CNpy | 476 | 21.0[g] | 388 | 25.8[h] | 398 | 6320 | 25.1 | 25.2 | 20.7 |
| **8** | $Mebpy^+$ | 532 (520)[d] | 18.8 | 426 | 23.5[f] | 444 | 7175 | 22.5 | 22.1 | 17.3 |
| **9** | pdz | 440 | 22.7[e] | 363 | 27.5[e] | 376 | 6070 | 26.6 | 26.8 | 22.9 |
| **10** | dmpz | 440 | 22.7[i] | 364 | 27.5[i] | 372 | 6590 | 26.9 | 26.9 | 22.9 |
| **11** | 2-Mepz | 449 | 22.3[e] | 362 | 27.6[e] | 380 | 6420 | 26.3 | 26.5 | 22.3 |
| **12** | pz | 454 (452)[d] | 22.0 | 372 (368)[e] | 26.9[f] | 386 | 6435 | 25.9 | 26.1 | 21.9 |
| **13** | pzO | 518 | 19.3[j] | 410 | 24.4[f] | 426 | 6810 | 23.5 | 23.5 | 19.4 |
| **14** | $dmpzH^+$ | 600 | 16.7[i] | 478 | 20.9[i] | 488 | | 20.5 | 20.5 | 16.1 |
| **15** | $pzH^+$ | 636 (625)[e] | 15.7[k] | 500 (490)[e] | 20.0[k] | 514 | | 19.5 | 19.4 | 14.8 |
| **16** | $Mepz^+$ | 655 | 15.1[d] | 524 | 19.1[e] | 532 | 14970 | 18.8 | 18.9 | 14.2 |

[a] This work, unless otherwise indicated. [b] Maximum of the asymmetric band. [c] Obtained by Gaussian deconvolution. [d] Reference 3. [e] Reference 9b. [f] Solutions of the Ru(II) complexes were obtained similarly to the Os(II) analogs (see text). [g] Reference 22. [h] Reference 12c. [i] Reference 23. [j] Reference 24. [k] Reference 25.

combining a standard three-electrode arrangement with a quartz cuvette, allowing for simultaneous determination of potential and spectra. The solutions of the Os(II) complexes (ca. $10^{-4}$ M) were also oxidized chemically with permanganate or with peroxydisulfate (in the latter case, using traces of $[Ru(NH_3)_5pz]^{2+}$ as a catalyst). A further reduction to the original Os(II) complexes was achieved by reaction with ascorbic acid.

Dissociation kinetic experiments with $[Os^{II}(CN)_5pz]^{3-}$ were carried out at $I = 0.5$ M (NaCl) using dmso as a scavenger ligand. Stoppered flasks containing several solutions with fixed amounts of the pz complex ($1 \times 10^{-4}$ M) and free pz ($5 \times 10^{-4}$ M) and increasing concentrations of dmso (up to 0.3 M) were kept at $60 \pm 1$ °C in a thermostated bath. The progress of the reaction was followed through the decrease of absorption at 386 nm, the maximum of $[Os^{II}(CN)_5pz]^{3-}$. The data were fitted to a single first-order decay.

## Results

**Visible−UV Spectra of the Os(II) Complexes.** Figure 1 shows the spectra for three members of the $[Os^{II}(CN)_5L]^{n-}$ series (L = py, pz, $Mepz^+$). The energy maxima and molar absorbances of the most intense bands in the visible region are shown in Table 1, together with data for other derivatives. It can be seen that the energies of the bands in the far-UV region (ca. 200 nm) are insensitive to L, while the bands at 234, 255, and 276 nm for L = py, pz, and $Mepz^+$, respectively ($\epsilon$ = ca. $5 \times 10^3$ $M^{-1}$ $cm^{-1}$), are similar in energy and intensity to those found for the corresponding free ligands (256, 262, and 274 nm). Weak shoulders appear on the low-energy side of the intense UV band, at 264, 290, and 335 nm for the three ligands, ordered as before. The energies of the asymmetric bands in the visible−near-UV region are strongly dependent on L; thus, the energy decreases as the acceptor ability of L increases.

A specific feature of the $[Os^{II}(CN)_5L]^{n-}$ complexes (not found for the Fe(II) and Ru(II) analogs) is the appearance of a shoulder in the low-energy side of the intense visible band, which clearly shows as a new band for the $[Os(CN)_5Mepz]^{2-}$ complex (Figure 1). Using the data of Table 1, a linear plot of the energy of the low-energy band against the high-energy one (slope $1.02 \pm 0.02$) shows that the differences in energy between both transitions are nearly constant throughout the series (ca. 4800 $cm^{-1}$). The intensities of the low-energy bands are lower than those for the main transition by a factor of about 2−4. Table 1 also shows that when L is changed, the molar absorbances increase in parallel with the decrease in energy; this is borne out by both the pyridine and the pyrazine derivatives.

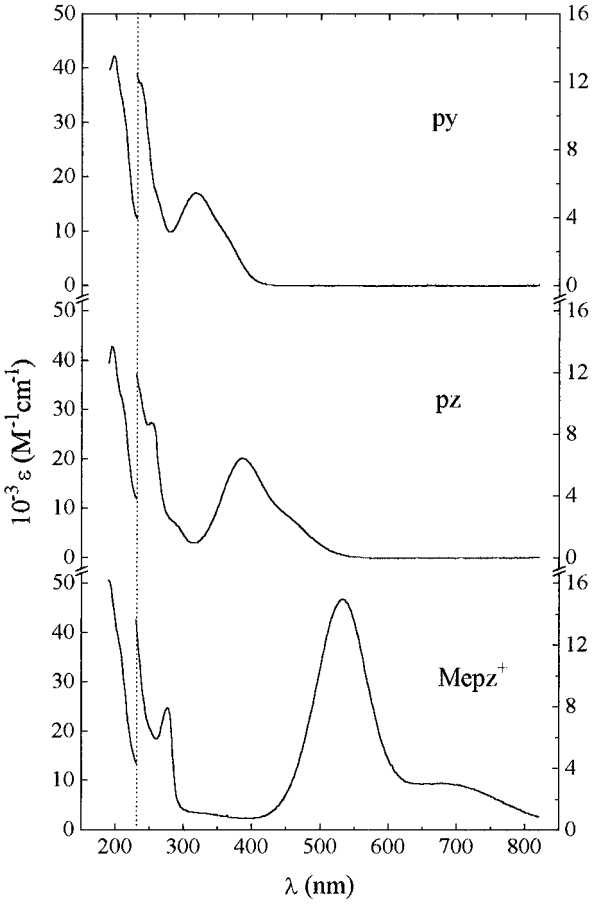


**Figure 1.** Electronic spectra of $[Os^{II}(CN)_5L]^{n-}$ complexes with L = py, pz, $Mepz^+$ in aqueous solution.

When the $[Os(CN)_5pz]^{n-}$ complex is dissolved in different organic solvents, strong solvatochromic shifts are detected. Figure 2 shows the behavior of both transitions. The intense bands in the visible region shift linearly to lower energies as

(22) Szeczy, A. P.; Miller, S. S.; Haim, A. *Inorg. Chim. Acta* **1978**, *28*, 189.
(23) Toma, H. E.; Stadler, E. *Inorg. Chem.* **1985**, *24*, 3085.
(24) Morando, P. J.; Bruyere, V. I. E.; Blesa, M. A.; Olabe, J. A. *Transition Met. Chem.* **1983**, *8*, 99.
(25) Slep, L. D.; Pollak, S.; Olabe, J. A. To be submitted.

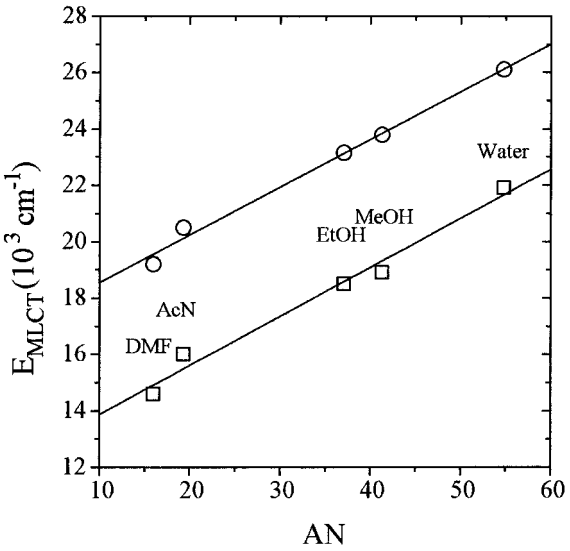


**Figure 2.** Plot of $E_{MLCT}$ for both transitions in $[Os(CN)_5pz]^{3-}$ against solvent acceptor number, AN (Gutmann's scale).

**Table 2.** Half-Wave Potentials (V *vs* NHE) for the $[M^{III/II}(CN)_5L]^{(n-1)-/n-}$ Couples (M = Os, Fe) and p$K_a$ Values for the Free L Ligands in Aqueous Solution

| ligand | $E_{1/2}$ (Os)[a] | $E_{1/2}$(Fe) | p$K_a$ |
|---|---|---|---|
| 4-Mepy | 0.63 | 0.45[b] | 6.02[c] |
| 3-Mepy | 0.66 | 0.46[d] | 5.68[c] |
| py | 0.65 | 0.47[b] | 5.25[c] |
| bpy | 0.69 | 0.51[d] | 4.44[a] |
| isn | 0.69 | 0.50[b] | 3.65[b] |
| Mebpy$^+$ | 0.70 | 0.54[d] | 4.14[a] |
| 4-CNpy | 0.72 | 0.53[e] | 1.90[f] |
| pdz | 0.69 | 0.53[d] | 2.24[c] |
| dmpz | 0.73 | 0.54[g] | 1.90[h] |
| 2-Mepz | 0.76 | 0.58[d] | 1.45[h] |
| pz | 0.78 | 0.63[i] (0.55)[b] | 0.65[h] |
| Mepz$^+$ | 0.96 | 0.79[b] | −5.8[b] |

[a] This work, $I = 0.1$ M ($NaNO_3$), $T = 25$ °C. [b] Reference 28, $I = 1$ M. [c] Reference 29. [d] This work, $I = 1$ M. [e] Reference 7e. [f] Reference 30. [g] Reference 23. [h] Reference 31. [i] Reference 32.

the acceptor number of the solvent (measured on the Gutmann scale)[26] decreases, with a slope of $(0.17 \pm 0.01) \times 10^3$ cm$^{-1}$/AN.

**Electrochemical Measurements. (a) Redox Potentials of the Os(III,II) Couples.** Typical cyclic voltammograms for the pyrazine derivative show a one-electron, reversible behavior (Supporting Information).[27] Table 2 shows the half-wave potentials for the different complexes, which also behave reversibly; the values roughly increase with the reducibility of the L ligand. The values for the iron analogs are included for the sake of comparison.

**(b) Reduction of the Mepz$^+$ Ligand.** The cyclic voltammograms for $[Os(CN)_5Mepz]^{2-}$ in aqueous solution also show a reversible behavior. This is not the case for the ruthenium analog; although the difference in peak potentials for the reduction and oxidation waves is 60 mV, the relative height of the latter decreases upon lowering the scan rate, which also influences the value of the half-wave potential; as the scan rate increases, a trend to reversible behavior is observed. For the iron complex, the irreversibility is greater, as no back-oxidation wave is detected. For the three complexes, as well as for free *N*-methylpyrazinium iodide, the reduction potentials were also measured by square-wave voltammetry; these values are displayed in Table 3.

**UV−Vis Spectra of the Os(III) Complexes.** Through the stepwise electrochemical oxidation of $[Os^{II}(CN)_5pz]^{3-}$, the intense absorption centered at 386 nm disappears and new absorptions appear at 388, 412, and 450 nm, with net isosbestic points at 263 and 341 nm. In addition, the band at 254 nm shifts to lower energy (Supporting Information, including the spectra of $[Os^{II}(CN)_5pz]^{3-}$ and $[Os^{III}(CN)_5pz]^{2-}$, obtained by factor analysis procedures).[33] Similar results are observed for other members of the series (no significant shifts of the visible bands are detected upon changing L). The Os(III) complexes are stable for at least 3 h, with the exception of the Mepz$^+$ derivative, which decomposes on the minute time scale.

**IR Spectra.** The wavenumbers for complexes with some selected L ligands (Supporting Information) show that the vibrations associated with L (800−1600 cm$^{-1}$) do not vary significantly with respect to the free ligand values. Similar splitting patterns of the intense C−N stretching and Os−C−N bending vibrations were found around 2050 and 550 cm$^{-1}$, respectively, compared to the one found for $Os(CN)_6^{4-}$.[13a] However, the latter species does not show the weak peak at ca. 2100 cm$^{-1}$, which appears in all the spectra of the pentacyano(L)osmate complexes.

**Dissociation Kinetics of the Pyrazine Ligand.** The dependence of $k_{obs}$ values (s$^{-1}$) on the concentration of the scavenger ligand, dmso, shows a saturation behavior (Supporting Information). At the saturation limit, $k_{obs} = 1.7 \times 10^{-6}$ s$^{-1}$ (60 °C).

## Discussion

**Synthetic Strategy.** As shown recently,[14] the $[Os(CN)_5L]^{n-}$ complexes can be obtained through the photochemical activation of $[Os(CN)_6]^{4-}$ in the presence of excess of ligand L.[34] If $[Os(CN)_5NO]^{2-}$ is used as a starting reagent, the release of $NO^+$ can be achieved through the reaction with bases such as $OH^-$ or hydrazine, followed by adduct decomposition and final coordination of L into the intermediate $[Os(CN)_5H_2O]^{3-}$ ion. Scheme 1 (Supporting Information) shows the alternative synthetic routes used in the present work.

**Infrared Spectra of the Os(II) Complexes.** The intense, split band around 2050 cm$^{-1}$ is characteristic of C−N stretching is osmium(II) cyanide complexes, as found with $[Os(CN)_6]^{4-}$.[13a] The same can be said of the bending Os−C−N absorption at ca. 550 cm$^{-1}$. The weak peak at ca. 2100 cm$^{-1}$ observed for the $[Os(CN)_5L]^{n-}$ complexes is presently assigned to the axial cyanide stretching mode; the shift of the latter to higher wavenumbers compared to the intense equatorial modes reflects the depletion of electron density at the axial $\pi^*$(CN) orbital because of the stronger electron-withdrawing ability of L, if compared with cyanide. The axial mode was also found at higher wavenumbers than equatorial modes of $[Os(CN)_5NO]^{2-}$;[14] this was confirmed by theoretical calculations.[35] Weak bands at ca. 2100 cm$^{-1}$ were also found for $[Fe(CN)_5pz]^{3-}$ and for

(26) Gutmann, V. *The Donor-Acceptor Approach to Molecular Interactions*; Plenum: New York, 1980.
(27) Bard, A. J.; Faulkner, L. R. *Electrochemical Methods*; Wiley: New York, 1980.
(28) Toma, H. E.; Creutz, C. *Inorg. Chem.* **1977**, *16*, 545
(29) *CRC Handbook of Chemistry and Physics*, 75th ed.; CRC Press, Inc.: Boca Raton, FL, 1994.
(30) Mason, S. F. *J. Chem. Soc.* **1959**, 1247.
(31) Chia, A. S.; Trimble, R. F. *J. Phys. Chem.* **1961**, *65*, 863.
(32) Moore, K. J.; Lee, L.; Mabbott, G. A.; Petersen, J. D. *Inorg. Chem.* **1983**, *22*, 1108.
(33) Parise, A. R.; Pollak, S.; Slep, L. D.; Olabe, J. A. *An. Asoc. Quim. Argent.* **1995**, *83*, 211.
(34) Balzani, V.; Carassiti, V. *Photochemistry of Coordination Compounds*; Academic: New York, 1970.
(35) Estrin, D. A.; Baraldo, L. M.; Slep, L. D.; Barja, B. C.; Olabe, J. A.; Paglieri, L.; Corongiu, G. *Inorg. Chem.* **1996**, *35*, 3897.

**Table 3.** Correlation between Optical Charge Transfer Energies ($E_{MLCT}$) and Electrochemical Potentials for the $M^{III,II}$ ($E_{ox}$) and $Mepz^{I,0}$ ($E_{red}$) Couples of the $[M(CN)_5Mepz]^{2-}$ ions (M = Fe, Ru, Os) in Aqueous Solution

| | | | | $E_{MLCT}(exp)^b$ | | $E_{MLCT}(corr)^c$ | |
|---|---|---|---|---|---|---|---|
| complex | $E_{ox}{}^a$ | $E_{red}{}^a$ | $E_{ox} - E_{red}$ | $\lambda$ (nm) | $E$ (eV) | (eV) | $\chi^d$ (eV) |
| $[Fe^{II}(CN)_5Mepz]^{2-}$ | 0.79[e] | −0.53 | 1.32 | 655[e] | 1.89 | 1.89 | 0.57 |
| $[Ru^{II}(CN)_5Mepz]^{2-}$ | 1.24 | −0.52 | 1.76 | 524[f] | 2.37 | 2.29 | 0.53 |
| $[Os^{II}(CN)_5Mepz]^{2-}$ | 0.96 | −0.54 | 1.50 | 532 | 2.33 | 2.14 | 0.64 |

[a] V *vs* NHE, $I = 0.1$ M ($NaNO_3$). Value of $E_{red}$ for *N*-methylpyrazinium iodide, −0.54 V. [b] Maxima of the visible MLCT bands (most intense one for Os). [c] Calculated as $E_{MLCT}(exp) - {}^1/_2\lambda$ with $\lambda_{Ru} = 1200$ cm$^{-1}$ and $\lambda_{Os} = 3200$ cm$^{-1}$. [d] According to eq 1; see text. [e] Reference 3. [f] Reference 9b.

$[Ru(CN)_5pz]^{3-}$,[9a] but not for the $[Os(CN)_5N_2H_5]^{2-}$ ion; in the latter case, the hydrazinium ligand does not compete for the $\pi$-electron density with cyanides and the axial and equatorial modes appear at close wavenumbers (2041 cm$^{-1}$).

**Electronic Spectra of the Os(II) and Os(III) Complexes**. We assign the spectra in Figure 1 as follows: the band at ca. 200 nm corresponds to a $d\pi(Os) \rightarrow \pi^*(CN)$ MLCT transition, as in the $[Os(CN)_6]^{4-}$ [36] and $[Os(CN)_5NO]^{2-}$ [14] ions, and the peaks in the 230−280 nm region correspond to intraligand $\pi$-(L) $\rightarrow \pi^*$(L) transitions, by comparison with the corresponding free-ligand values.[37] No clear assignments can be made for the weak absorptions at 264, 290, and 335 nm (see below, however). Finally, the main peak in the broad visible−near-UV absorption is assigned to a $d\pi(Os) \rightarrow \pi^*$(L) MLCT transition, on the basis of the following conclusive evidence: (i) The intense absorptions disappear upon oxidation to Os(III) and are recovered upon immediate reduction. (ii) The energy depends on the reducibility of L. Table 1 shows that the type and position of the substituents on a given ring influence the MLCT energies in the expected way, by determining the energy of the $\pi^*$(L) orbital, as also shown for complexes of related series.[3,9] (iii) The nature of the "auxiliary" coligands influences the energy of the Os(II) ground state; the $Os^{II}(CN)_5L^{n-}$ complexes display the energy maxima at higher energies than the corresponding $Os^{II}(NH_3)_5L^{n+}$ complexes,[38] because of the strong stabilization of the $d\pi(Os)$ orbitals through the competitive $\pi$ interactions with cyanides. (iv) The onset of strong solvatochromic effects (Figure 2) is observed. The trends are the same as previously observed for the pentacyano(L)ferrate(II) complexes,[39] resulting from the strong, specific interactions between donor cyanides and the acceptor solvent. The slope in Figure 2 for $[Os(CN)_5pz]^{3-}$ ($0.17 \times 10^3$ cm$^{-1}$/AN) is significantly greater than the one found for $[Fe(CN)_5pz]^{3-}$, $0.10 \times 10^3$ cm$^{-1}$/AN. The difference measures the higher sensitivity of the osmium complex toward changes in the acceptor ability of the solvent, arising in the stronger $\pi$-donor ability of osmium *vs* iron when interacting with cyanides.[40] (v) By comparing data from Table 1 with values for the $[Fe^{II}(CN)_5L]^{n-}$ [2,3] and $[Ru^{II}(CN)_5L]^{n-}$ [9] series, one can see that the energy shifts for the three $[M^{II}(CN)_5L]^{n-}$ series are similar when the L ligands are changed. The plots of $E_{MLCT}$ for the members of the $[M(CN)_5L]^{n-}$ series (M = Fe, Ru) against the energy for the corresponding $[Os(CN)_5L]^{n-}$ complexes (Supporting Information) were rigorously linear, with slopes of 0.98 ± 0.02 and 0.99 ± 0.03, respectively. This result confirms the MLCT assignment and also shows that the metal−cyanide interaction is dominant in the overall bonding scheme for the three metal series; moreover, it suggests that the degree of M−L back-bonding is roughly the same for the three metal centers.[41] (vi) For the $[Os^{II}(CN)_5L]^{n-}$ series, the increase in molar absorbance of the MLCT bands with the acceptor ability of the L ligand is indicative of a significant degree of mixing in the ground and excited states.[3]

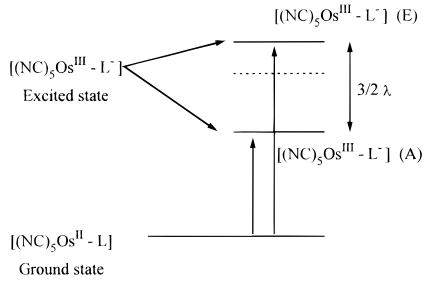


**Figure 3.** Splitting of the MLCT excited state in $[Os(CN)_5L]^{n-}$ under spin−orbit coupling.

Considering that the difference in energy between the two transitions in $[Os(CN)_5L]^{n-}$ remains constant for any L ligand, we assign them to spin−orbit split components of the MLCT band. No splitting was observed with the $[Fe^{II}(CN)_5L]^{n-}$ complexes; with the $[Ru^{II}(CN)_5pz]^{3-}$ ion, however, a broadening at the low-energy side of the MLCT band can be appreciated,[9a] in agreement with the intermediate value of the spin−orbit coupling constant for ruthenium (reported values of the constant, $\lambda$, are ca. 400, 1200, and 3200 cm$^{-1}$ for iron, ruthenium, and osmium, respectively).[42] Similar distinctive spectral patterns have been observed for Os(II)−polypyridine complexes.[43]

Although the low-spin $d^6$ configuration is not split under spin−orbit coupling effects, the excited-state $d^5$ configuration leads to the A and E states, according to the simplified model,[44] shown in Figure 3. In this interpretation, two transitions should be observed with an energy difference of ${}^3/_2\lambda$, the lower energy one being of approximately half-intensity. The intensities in Figure 1 are almost as predicted, and from the difference in energies between both transitions, we calculate $\lambda = 3200$ cm$^{-1}$, in good agreement with reported values. This splitting pattern was proposed for interpreting the spectral results arising from

(36) Lever, A. B. P. *Inorganic Electronic Spectroscopy*, 2nd ed.; Elsevier: Amsterdam, The Netherlands, 1984.
(37) The blue shifts in the energy of the $\pi \rightarrow \pi^*$ intraligand band upon coordination to Os(II) (which are seen for all the L ligands except $Mepz^+$) seem to reflect the predominant increase in the energy of the $\pi^*$ level (due to back-bonding interactions) compared to the changes in the ground-state $\pi$ level.
(38) (a) Sen, J.; Taube, H. *Acta Chem Scand., Ser. A* **1979**, *A33*, 125. (b) Magnuson, R. H.; Taube, H. *J. Am. Chem. Soc*. **1975**, *97*, 5129. (c) Lay, P. A.; Magnuson, R. H.; Taube, H. *Inorg. Chem*. **1988**, *27*, 2848.
(39) Toma, H. E.; Takasugi, M. S. *J. Solution Chem.* **1983**, *12*, 547.
(40) Garcia Posse, M. E.; Katz, N. E.; Baraldo, L. M.; Polonuer, D. D.; Colombano, C. G.; Olabe, J. A. *Inorg. Chem.* **1995**, *34*, 1830.
(41) A discussion on the significance of the slope values for the $E_{MLCT}$ plots can be found in ref 9b. Thus, a low value ($p$ = ca. 0.5) in the $[Os(NH_3)_5L]^{n+}$/ $[Fe(CN)_5L]^{n-}$ correlation was indicative of a strong Os−L back-bonding interaction (ca. 54% ligand character for L = pz). Values of $p = 0.8$ and 0.9 for the $[Ru(NH_3)_5L]^{n+}$/$[Fe(CN)_5L]^{n-}$ and $[Ru(CN)_5L]^{n-}$/$[Fe(CN)_5L]^{n-}$ plots, respectively, suggested a decreasing back-bonding to L for the ruthenium derivatives when ammonia is replaced by cyanide (from ca. 20% to 9%). From the previous and present results, we conclude that a 7−10% ligand character is present for the three $[M^{II}(CN)_5L]^{n-}$ complexes.
(42) Goodman, B. A.; Raynor, J. B. *Adv. Inorg. Radiochem.* **1970**, *13*, 192.
(43) Kober, E. M.; Meyer, T. J. *Inorg. Chem*. **1982**, *21*, 3967.
(44) Curtis, J. C.; Meyer, T. J. *Inorg. Chem*. **1980**, *19*, 3833.

the outer-sphere intervalence transitions with the hexacyanide species as donors and Ru(III) complexes as acceptors. According to a more elaborate treatment,[45] the low symmetry at the osmium site should lead to *three* transitions with intensity ratio 0.30:0.58:0.11; the results for the $[Os(CN)_5L]^{n-}$ spectra in Table 1 would correspond to the first two transitions, while the third one could be assigned to the shoulders appearing at the low-energy side of the intense UV band (see Results).

A quantitative relationship between $E_{MLCT}$ and the measured redox potentials for metal oxidation, $E_{ox}$, and ligand L reduction, $E_{red}$, was established for a series of ruthenium polypyridine complexes, as shown by eq 1.[46] By applying this equation to

$$E_{MLCT} = (E_{ox} - E_{red}) + \chi \qquad (1)$$

the three metal pentacyano complexes with L = $Mepz^+$, we obtain the results shown in Table 3. In eq 1, $E_{MLCT}$ corresponds to the HOMO → LUMO transition, which is a vertical process in the Franck−Condon sense; *i.e.*, transitions occur between potential energy surfaces at the unchanged ground state geometry. The difference between $E_{ox}$ and $E_{red}$ corresponds to the HOMO−LUMO energy difference in the relaxed state (energy potential minima). Thus, $\chi$ includes contributions from intramolecular relaxation and solvent reorganization after MLCT excitation.[46] In Table 3, $\chi$ shows a greater value than those found for ruthenium(II) polyazine complexes (ca. 0.3 eV)[47] and close to the ones observed for other complexes with extensive reorganization energies (ca. 0.6−0.7 eV).[48] In the cyanide complexes, the reorganization can be significant, as changes in the specific interactions of cyanides with solvent are operative upon going to the excited state (the metal acquires some III character and cyanides become more acidic).[49]

The bands of the Os(III) complexes are assigned to LMCT transitions from cyanides to Os(III); thus, the energies are almost independent of the changes in L, including the spectrum of the $[Os(CN)_6]^{3-}$ ion.[36] In contrast with the results found for the Os(II) complexes, the shift to lower energy of the $\pi \rightarrow \pi^*$ transition upon complexation to Os(III) is consistent with the electrostatic stabilization of the $\pi^*$ level (this is equivalent to protonation of the L ligand).

**Redox Potentials.** Table 2 shows that the redox potentials of the Os(III,II) couples depend on L similarly to those of the iron[2] and ruthenium complexes.[50] The Os(II) ground state is stabilized upon going from $[Os(CN)_6]^{4-}$ ($E_{1/2}$ = 0.64 V) to the pentacyanide−L species, the difference being greater as L becomes a stronger electron-withdrawing ligand, which means a stronger $\pi$-acceptor as well as a weaker $\sigma$-donor.[51] In fact, Figure 4a shows that $E_{ox}$ depends in a linear way on the p$K_a$ of the L ligands. The variation of $E_{ox}$ with L follows a trend similar to that for the iron analog complexes; Figure 4b shows a linear plot of $E_{ox}$(Fe) against $E_{ox}$(Os), with slope 1.06 ± 0.05; this is as expected, in view of the previously discussed correlation of the $E_{MLCT}$ energies.

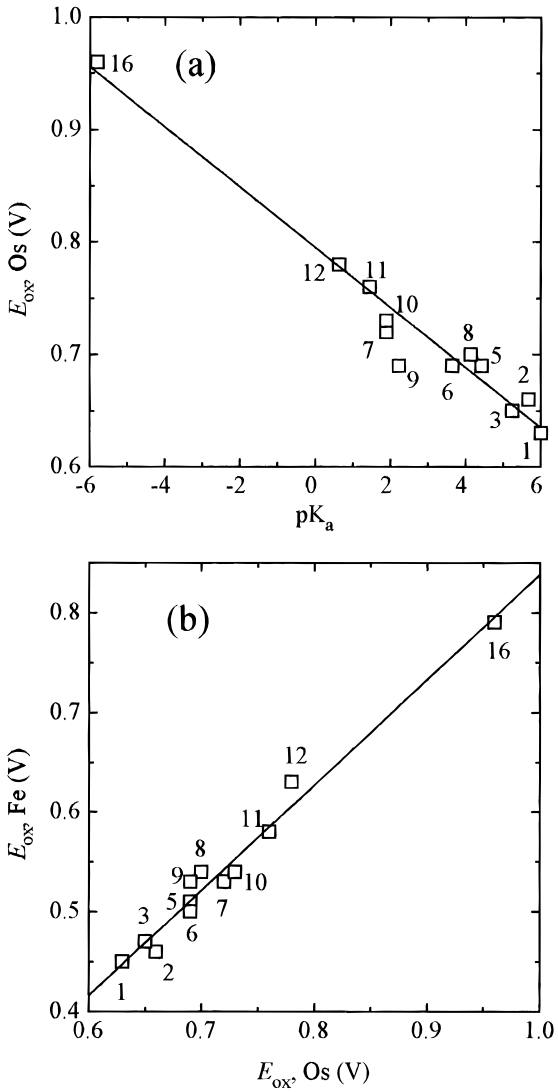


**Figure 4.** (a) Correlation between the potentials of the $Os^{III,II}$ redox couple in $[Os(CN)_5L]^{n-}$ complexes, $E_{ox}$, and the p$K_a$ of the free ligands. (b) Correlation between $E_{ox}$(Fe) and $E_{ox}$(Os) for several L ligands. Each data point is numbered according to the ligand as identified in Table 1.

The values of $E_{red}$ in Table 3 for the three $[M(CN)_5Mepz]^{2-}$ complexes are nearly independent of the metal and are also close to the value for free $Mepz^+$. As $E_{red}$ is a direct measure of the energy of the LUMO, and considering that the latter should be diminished upon coordination because of electrostatic stabilization,[51] we conclude that a compensating effect arising in back-bonding to the $Mepz^+$ ligand is operative. Moreover, the results confirm that the degrees of back-bonding must be almost the same for the three metals, in agreement with our previous results and interpretations.

**Dissociation Kinetics.** The stoichiometry of the dissociation of pyrazine from $[Os(CN)_5pz]^{3-}$ is described by eq 2. The decrease in concentration of $[Os(CN)_5pz]^{3-}$ is coupled to the

(45) Kober, E. M.; Goldsby, K. A.; Narayana, D. N. S.; Meyer, T. J. *J. Am. Chem. Soc.* **1983**, *105*, 4303.

(46) (a) Dodsworth, E.; Lever, A. B. P. *Chem. Phys. Lett.* **1985**, *119*, 61. (b) Dodsworth, E.; Lever, A. B. P. *Chem. Phys. Lett.* **1986**, *124*, 152. In fact, the $E_{red}$ value considered in eq 1 corresponds to the reduction of L in the presence of a Ru(III) center. Experimental values of $E_{red}$, however, are measured in the presence of M(II) centers; the latter can be used because both $E_{red}$ values are related by a solvational energy term, which remains constant for the whole series and may be included in $\chi$ (cf. also ref 40).

(47) Ernst, S. D.; Kaim, W. *Inorg. Chem.* **1989**, *28*, 1520.

(48) Hilgers, F.; Brun, W.; Fiedler, J.; Kaim, W. *J. Organomet. Chem.*, in press.

(49) In Table 3, the quoted values of $\chi$ appear as a result of a correction made to the $E_{MLCT}$ values for the ruthenium and osmium complexes, because of spin−orbit coupling effects. This was not the case for iron, as no band asymmetry was found, and thus the measured maximum energy corresponds to the unsplit case, *i.e.* the weighted average of the A and E states (see Figure 3). For osmium, however, the high-energy component (transition to the E state) must be diminished by $^1/_2\lambda$ in order to obtain an energy value free of spin−orbit effects. The same subtraction was performed for the ruthenium complex.

(50) Redox potential values for the $[Ru(CN)_5L]^{n-}$ series are scarce in the literature (cf. ref 10). Our measurements for several L ligands show a trend similar to those found for iron and osmium complexes.

(51) Crutchley, B. J.; Lever, A. B. P. *Inorg. Chem.* **1982**, *21*, 2276.

$$[Os^{II}(CN)_5pz]^{3-} + dmso \rightleftharpoons [Os^{II}(CN)_5dmso]^{3-} + pz \quad (2)$$

formation of a very stable complex, $[Os(CN)_5dmso]^{3-}$, which absorbs in the UV region. The dependence of $k_{obs}$ on the concentration of the entering ligand, dmso, is as already found for $[Fe(CN)_5L]^{n-}$ [3] and $[Ru(CN)_5L]^{n-}$ [11b] complexes. The saturation kinetics provides a direct measurement of $k_{-pz}$, the specific dissociation rate constant for pyrazine release according to a dissociative mechanism, as described elsewhere.[2,3] By comparison with values of $k_{-pz}$ for $[Fe(CN)_5pz]^{3-}$, $4.2 \times 10^{-4}$ $s^{-1}$, and $[Ru(CN)_5pz]^{3-}$, $1.77 \times 10^{-5}$ $s^{-1}$,[3,11b] it can be seen that the estimated value for $[Os(CN)_5pz]^{3-}$ is much lower, ca. $2.0 \times 10^{-8}$ $s^{-1}$ (25 °C).[52] As the degrees of back-bonding to a given L ligand appeared to be very similar for the three metals, we consider that the difference could be related to the stronger $\sigma$ interaction at the Os−pz bond, as a result of an increasing overlap on going from iron to ruthenium and osmium.[15,53,54] The onset of strong $\sigma-\pi$ interactions was recently discussed for the $[Os(CN)_5NO]^{2-}$ ion.[14] A more detailed kinetic and mechanistic study for the dissociation of pyrazine and other L ligands is underway.

## Conclusion

A new series of osmium cyanide complexes presents a bonding picture similar to that found previously for the analogous iron and ruthenium series, as shown by the shifts in energy (and intensity) of the MLCT bands with the changes in electron-withdrawing ability of the L ligand. The greatest $\pi$-donor ability of osmium is manifested mainly through the strong, dominant interaction with cyanides. The degrees of back-bonding to a given L ligand appear to be roughly the same for the three metal analogs. In contrast, the $\sigma$ interaction at the Os−L bond seems to be much stronger than the analogous interactions for iron and ruthenium, as suggested by the kinetic dissociation results. The influence of spin−orbit coupling effects for the osmium complexes (and, to a lower degree, for ruthenium) is revealed in the splitting of the MLCT bands. The new series turns out to be of strategic value for further mechanistic studies on electron transfer reactions, as well as for using the $[Os(CN)_5L]^{n-}$ complexes for creating new series of binuclear or polynuclear supramolecular assemblies. The high stability of $Os^{II}-L$ and $Os^{III}-L$ bonds toward dissociation, the expected high $k_{exch}$ values for the $[Os^{II}(CN)_5L]^{n-}/[Os^{III}(CN)_5L]^{(n-1)-}$ reactions (suggested by the recent results on the $[Os(CN)_6]^{4-}/[Os(CN)_6]^{3-}$ system),[13c] and the ubiquitous redox potential range displayed by the complexes with different L's seem to be particulary noteworthy for extending systematic studies on the coordination chemistry of the $X_5M-L$ systems.

**Acknowledgment.** Our thanks are expressed to the University of Buenos Aires (UBA), to the Consejo Nacional de Investigaciones Científicas y Técnicas (Conicet), and to the Deutsche Gesellschaft für Technische Zusammenarbeit Gmbh for financial support. L.D.S. is a member of the Fellowships Program (UBA), and J.A.O. is a member of the scientific staff of Conicet.

**Supporting Information Available:** A chart listing abbreviations used for the ligands, a table containing selected IR data, figures containing cyclic voltammograms for $Os^{III,II}$ and $Mepz^{+/0}$ redox couples, spectroelectrochemical conversion of $[Os^{II}(CN)_5pz]^{3-}$ into $[Os^{III}(CN)_5pz]^{2-}$, a plot of the pseudo-first-order dissociation rate constant against dmso concentration for the $[Os^{II}(CN)_5pz]^{3-}$ ion, and plot of $E_{MLCT}$(Fe and Ru) against $E_{MLCT}$(Os), and Scheme 1, giving the procedures used for preparing the $[Os(CN)_5L]^{n-}$ complexes (8 pages). Ordering information is given on any current masthead page.

IC960377Z

(52) Only a rough estimation of $k_{-pz}$ at 25 °C is presently reported; this was done by using the value of $k_{-pz}$ at 60 °C and assuming an Arrhenius type behavior with $E_{act} = 25$ kcal/mol.

(53) Williams, A. F. *A Theoretical Approach to Inorganic Chemistry*; Springer-Verlag: Berlin, Heidelberg, Germany, New York, 1979; p 255.

(54) As suggested by a reviewer, the strongest $\sigma$ interaction of L at the osmium center could also be traced to the partial "$M^{III}$" character made available by the $\pi$-acid ability of cyanides. This is consistent with the relative solvatochromic changes of the MLCT bands, showing that Os is the strongest $\pi$-donor.